ESC European Society of Cardiology

Cardiovascular Research (2018) **114**, 431–442
doi:10.1093/cvr/cvx245

Mitochondrial targeted peptides preserve mitochondrial organization and decrease reversible myocardial changes in early swine metabolic syndrome

Fang Yuan[1,2], John R. Woollard[1], Kyra L. Jordan[1], Amir Lerman[3], Lilach O. Lerman[1,3], and Alfonso Eirin[1]*

[1]Department of Medicine, Division of Nephrology and Hypertension, Mayo Clinic, Rochester, MN, USA;[2]Department of Cardiology, People's Hospital of Zhengzhou University, Henan Provincial People's Hospital, Henan, PR China; and [3]Department of Cardiovascular Diseases, Mayo Clinic, Rochester, MN, USA

Received 12 July 2017; revised 25 September 2017; editorial decision 21 November 2017; accepted 15 December 2017; online publish-ahead-of-print 18 December 2017

Time for primary review: 17 days

Aims The mechanisms responsible for cardiac damage in the early stages of metabolic syndrome (MetS) remain unknown. Mitochondria are intimately associated with cellular myofibrils, with the cytoskeleton functioning as a linkage coordinator, and closely associated to the calcium release sites of the sarcoplasmic reticulum (SR). We hypothesized that early MetS is characterized by mitochondria-related myocardial damage, associated with altered cytoskeletal–mitochondria–SR interaction.

Methods and results Domestic pigs were studied after 16 weeks of diet-induced MetS, MetS treated for the last 4 weeks with the mitochondrial-targeted peptide elamipretide (ELAM; 0.1 mg/kg SC q.d), or Lean controls ($n = 6$/group). Cardiac remodeling and function were assessed by fast comuted tomography. Myocardial mitochondrial structure, SR–mitochondria interaction, calcium handling, cytoskeletal proteins, oxidative stress, and apoptosis were studied *ex-vivo*. MetS pigs developed hyperlipidemia, hypertension, and insulin resistance, yet cardiac function was preserved. MetS-induced mitochondrial disorganization, decreased (C18:2)4 cardiolipin, disrupted ATP/ADP balance, and decreased cytochrome-c oxidase (COX)-IV activity. MetS also increased mitochondrial hydrogen peroxide (H_2O_2) production, decreased nicotinamide adenine dinucleotide phosphate (NADPH)/NADP and GSH/GSSG, and decreased myocardial desmin and β2 tubulin immunoreactivity, and impaired SR–mitochondrial interaction and mitochondrial calcium handling, eliciting myocardial oxidative stress and apoptosis. ELAM improved mitochondrial organization and cardiolipin species profile, restored ATP/ADP ratio and COX-IV activity, decreased H_20_2 production, and improved generation of NADPH and GSH. ELAM also improved cytoskeletal–mitochondria–SR interaction and mitochondrial calcium handling, attenuating oxidative stress, and apoptosis.

Conclusions Disorganization of cardiomyocyte cytoskeletal-mitochondria-SR network is associated with cardiac reversible changes in early MetS, preceding overt cardiac dysfunction. These findings may introduce novel therapeutic targets for blunting cardiac damage in early MetS.

Keywords Metabolic syndrome • Mitochondria • Myocardium • Cytoskeleton • Elamipretide

1. Introduction

The metabolic syndrome (MetS) is a group of cardiovascular risk factors that include obesity, insulin resistance, hypertension, and dyslipidemia. The prevalence of MetS is increasing at an alarming rate, leading toward a worldwide epidemic.[1] Advanced MetS induces myocardial damage, which increases cardiovascular morbidity and mortality,[2] yet the initial mechanisms responsible for triggering MetS-induced cardiac damage remain unknown.

* Corresponding author. Tel: +507 538 9941; fax: +507 266 9316, E-mail: eirinmassat.alfonso@mayo.edu

The heart is a high-energy demand organ that contains large numbers of mitochondria, organelles that play an important role in energy metabolism and other cellular process, such as generation of reactive oxygen species (ROS), cellular proliferation, and apoptosis. Structurally, cardiomyocyte mitochondria are arranged in packed strands that run between the myofibrils where they interact with cytoskeleton proteins, including desmin and β2 tubulin, which function as linkage coordinators.[3] Interactions between cytoskeletal proteins and the mitochondrial voltage-dependent anion channel (VDAC) are critical for controlling mitochondrial respiratory function and permeability.[4] Furthermore, cardiac mitochondria regulate calcium homeostasis through interconnections with the sarcoplasmic reticulum (SR), which support reciprocal calcium and ADP exchange. Mitochondrial calcium uptake activates the tricarboxylic acid (TCA) cycle and electron transport chain, contributing to antioxidant nicotinamide adenine dinucleotide phosphate (NADPH) regeneration and efficient energy production.[5] Therefore, mitochondrial alterations and disorganization may directly translate into myocardial damage and dysfunction.

Accumulating evidence indicates that mitochondrial abnormalities play a key role in the pathogenesis of myocardial remodeling and dysfunction associated with heart failure and ischemia/reperfusion injury.[6] We have recently shown that cardiac remodeling and impaired left ventricular (LV) relaxation in swine renovascular hypertension are partly attributable to cardiac mitochondrial damage, which is characterized by alterations in the inner mitochondrial membrane cardiolipin and impaired SR–mitochondria interactions.[7] Furthermore, rats with volume overload and LV dysfunction exhibit cardiomyocyte cytoskeletal abnormalities and mitochondrial damage, suggesting that disorganization of the cardiomyocyte cytoskeletal-myofibrillar-mitochondrial architecture may be a causative factor in the ultimate progression to heart failure.[8]

Cardiac dysfunction in murine models of MetS is associated with increased mitochondrial ROS formation and impaired oxidative phosphorylation capacity,[9,10] linking mitochondrial damage to MetS-induced heart failure. However, whether altered cytoskeletal–mitochondria–SR interactions are implicated in cardiac damage in the early stages of MetS, prior to development of overt cardiac dysfunction, remain unknown. In this study, we hypothesized that early swine MetS is characterized by mitochondrial disorganization and altered cytoskeletal–mitochondria–SR interaction, which can be blunted using mitoprotection with the mitochondrial-targeted peptide elamipretide (ELAM).

2. Methods

2.1 Study groups and experimental design

The study was approved by the Institutional Animal Care and Use Committee. Animal experiments were performed conform the NIH guidelines (Guide for the care and use of laboratory animals). Eighteen 3-month-old female domestic pigs were studied after 16 weeks of observation (*Figure 1A*). At baseline, pigs were randomized into two groups. Lean pigs ($n = 6$) were fed standard diet (13% protein, 2% fat, 6% fiber; Purina Animal Nutrition LCC, MN, USA), whereas MetS pigs ($n = 12$) were fed a high-fat/high fructose diet (5B4L; protein 16.1%, ether extract fat 43.0%, and carbohydrates 40.8%; Purina TestDiet, Richmond, IN, USA).[11]

Twelve weeks later, six MetS pigs started treatment with subcutaneous injections of ELAM (also known as Bendavia or MTP-131; Stealth BioTherapeutics, Inc., Newton Centre, MA, USA), 0.1 mg/kg in 1 mL of phosphate-buffered saline (PBS) once daily 5 days/week for the following 4 weeks.[7,12] A PBS vehicle was injected in the remaining six MetS and six Lean pigs.

Four weeks later, the pigs were anaesthetized with 0.25 g of intramuscular tiletamine hydrochloride/zolazepam hydrochloride and 0.5 g of xylazine, and anesthesia was maintained with intravenous ketamine (0.2 mg/kg/min) and xylazine (0.03 mg/kg/min).[13] Blood samples were collected, and cholesterol fractions and triglyceride levels were measured by standard procedures. Glucose and insulin levels were measured in fasting blood samples, and insulin resistance was calculated with the homeostasis model assessment of insulin resistance (HOMA-IR).[11] Cardiac remodeling and function were assessed using multi-detector computed tomography (MDCT). Arterial blood pressure was measured with an intra-arterial catheter during MDCT studies.

One week after completion of *in vivo* studies, pigs were euthanized with sodium pentobarbital (100 mg/kg IV Fatal Plus; Vortech Pharmaceuticals, Dearborn, MI, USA). Hearts were harvested and LV tissue sections frozen in liquid nitrogen, and maintained at -80 °C, or preserved in formalin for *ex vivo* studies.

2.2 Cardiac function

Cardiac function was assessed using MDCT (Somatom Sensation-128; Siemens Medical Solution, Forchheim, Germany) and images analyzed with the Analyze™ software package (Biomedical Imaging Resource, Mayo Clinic, MN, USA), as previously described.[14] The entire LV was scanned 20 times throughout the cardiac cycle to calculate ejection fraction. LV endocardial and epicardial borders were traced to calculate LV muscle mass (LVMM). Rate-pressure product (RPP) was calculated as heart rate times systolic blood pressure.

2.3 Mitochondrial content, morphology, and function

Myocardial mitochondrial number was examined by immunofluorescence staining with the mitochondrial outer membrane marker preprotein translocases of the outer membrane (TOM)-20 (Santa CruzBiotechnology, Dallas, TX, USA)[7] and quantified in 15–20 random fields using a computer-aided image analysis program (ZEN®2012 blue edition, Carl ZEISS SMT; Oberkochen, Germany). Mitochondrial morphology was assessed by transmission electron microscopy (Philips CM10 Transmission Electron Microscope, Philips Electron Optics, Eindhoven, The Netherlands). LV samples (2–3 mm^3) were fixed with Trump's fixative and processed at the Mayo Clinic's electron microscopy core facility. For analysis, five representative cardiomyocytes were randomly selected in each pig myocardium. Mitochondrial area and matrix density were measured using the National Institutes of Health Image-J software (version 1.44 for Windows). Only mitochondria fully contained within the borders of the transmission electron microscopy images were included in the analysis. In addition, five cross-sectioned cardiomyocytes per pig (a total of 30 cardiomyocytes per group) were randomly selected, and the number of subsarcolemmal mitochondria/cell counted and averaged.

Myocardial expression of cardiolipin synthase (CRLS)-1 was measured by western blot (Cat#ab156882; Abcam, Cambridge, MA, USA).[7] In brief, myocardial mitochondria were isolated using the MITO-ISO kit (Cat#8268; ScienCell, Carlsbad, CA, USA),[15] and standard western blotting protocols performed with specific previously used antibodies or those that cross-react with swine tissue. Frozen LV tissue was pulverized and homogenized. Then, the homogenized lysates from LV tissue were centrifuged, the supernatant removed, and the protein concentration determined by spectrophotometry. The lysate was then diluted in polyacrylamide gel electrophoresis sample buffer, sonicated, and heated to denature the proteins. Finally, the lysate was loaded onto a gel and

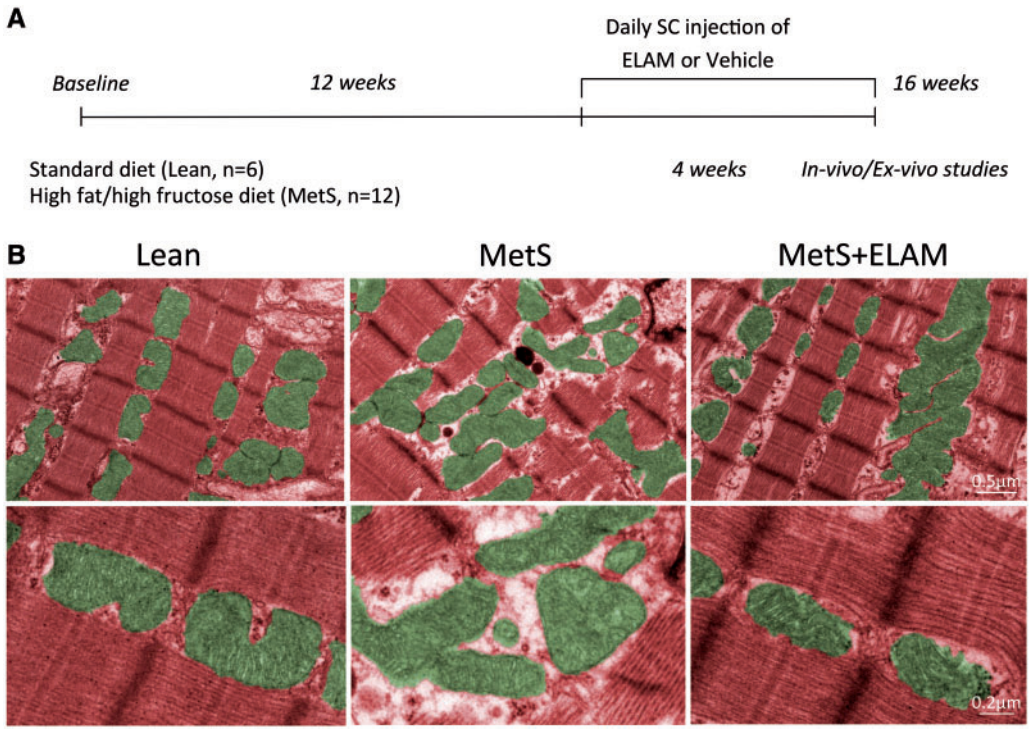

Figure 1 *MetS induced disorganization of cardiomyocyte mitochondria.* (*A*) Schematic of the experimental design. (*B*) Representative transmission electron microscopy images showing that MetS cardiomyocyte mitochondria (green) display loss of linear registry and clustering, associated with increased intracellular space, all of which were restored in MetS + ELAM-treated pigs ($n = 6$/group).

subsequently run with specific antibodies. Western blotting protocols were followed in each kidney sample using specific polyclonal antibodies against CRLS-1(Abcam; Cat#ab156882).[7] LV samples from all animals were homogenized using standard procedures.[16] Protein concentration was measured using bicinchoninic acid assay kit and bovine serum albumin standard curve. Western blotting analysis was carried out in a well membrane Criterion™ Precast; 4-15% Tris-HCl 1.0mm (Bio Rad, Hercules, CA, USA). Data were analyzed using Carestream Molecular Imaging Software (version 5.0.720).

Cardiolipin content and molecular composition were evaluated by mass spectrometry. Lipids were extracted from LV tissue using a chloroform/methanol solution (Bligh Dyer extraction), and individual lipid extracts reconstituted with chloroform: methanol (1:1), flushed with N_2, and stored at -20 °C for analysis. Enhanced multidimensional mass spectrometry-based shotgun lipidomics was performed, and total content and fractions of cardiolipin molecular species were quantified, as previously described.[12] Cardiolipin remodeling activity was assessed by mRNA expression of the cardiolipin regulators tafazzin (Taz)-1 and acyl-CoA: lysocardiolipin acyltransferase (ALCAT)-1.[12]

Myocardial expression of the cytochrome-c oxidase (COX) subunits I (abnova, Zhongli District, Taoyuan City, Taiwan; 1:1000, Cat# ab53766), II (abnova 1:1000, Cat# ab23672), III (LifeSpan BioSciences, Seattle, WA, USA; 1:1000, Cat# LS-C411664), and IV (Cell Signaling; 1:1000, Cat# 4850) was assessed by western blot. In addition, myocardial ATP and ADP content and COX-IV activity were assessed by colorimetric and fluorometric methods (Abcam; Cat# ab83355 and Abnova; Cat# KA3950, respectively).

Mitochondrial hydrogen peroxide (H_2O_2) production was measured by colorimetric quantitative methods (OxisResearch, BIOXYTECH®, Belmont, CA, USA H2O2-560™ Assay; Cat# 21024),[17] whereas mitochondrial antioxidant activity was assessed by the expression of superoxide dismutase (SOD)-1 (Abcam; Cat# ab16831), SOD-2 (Abcam; Cat# ab13533), thioredoxin (TRX)-2 (Abcam; Cat# ab185544), peroxiredoxin (PRX)-3 (Abcam; Cat# ab73349), as well as glutathione activity (glutathione (GSH)/GSSG; OxisResearch GSH/GSSG-412) and NADPH regeneration (NADPH/NADP Assay kit; Cat# ab65349; Abcam).

Mitochondrial dynamics was assessed by the expression of the fusion markers mitofusin (MFN)-1 (Abnova; Cat# H00055669-P01) and optic atrophy protein (OPA)-1 (Cat# 30573; Santa Cruz Biotechnology Inc., Dallas, TX, USA), and the fission markers mitochondrial fission factor (MFF; Abnova; Cat# PAB20518) and dynamin-related protein (DRP)-1 (Cell Signaing; Cat# 8570). Mitophagy was assessed by myocardial expression of p62 (Abcam; Cat# ab56416) and double immunofluorescence staining with Parkin (Santa Cruz; Cat# sc-13279) and Phosphatase and tensin homolog PTEN-induced putative kinase 1 (PINK)-1 (Sigma; Cat# MABN505).[15] The extent of Parkin-PINK-1 co-localization was assessed with the Mander's coefficient using Image-J (Colocalization Plugin) and reported as M1 (representing overlap between Parkin and PINK-1).

2.4 Cytoskeletal proteins and mitochondrial-SR interaction

Myocardial immunoreactivity and expression of the cytoskeleton proteins desmin (Bio-Genex, Fremont, CA, USa; clone 33, 1:40) and β2 tubulin (clone V9, 1:100; Sigma, St. Louis, MO, USA) were assessed by

double immunofluorescence staining with the cardiomyocyte marker connexin-43 (Abcam; Cat# ab79010) and western blot.

SR–mitochondrial interaction was assessed by immunofluorescence co-staining of the mitochondrial membrane using VDAC and the sarcoplasmic-reticulum marker ryanodine receptor (RYR). SR-mitochondria co-localization was assessed with the Mander's coefficient using Image-J, as we previously described.[7] Double immunofluorescence staining with the mitochondrial markers VDAC, and TOM-20, and the SR markers RYR and sarcoplasmic/endoplasmic reticulum calcium-ATPase (SERCA)-2a were performed to serve as controls. Mitochondrial calcium signaling was assessed by the expression of mitochondrial calcium uniporter (MCU; Abnova; Cat# H00090550-K).

2.5 Myocardial changes

Intramyocardial fat deposition was measured by Oil-red-O staining (Abcam; Cat#ab150678), and oxidative stress by *in situ* production of superoxide anion detected by dihydroethidium (DHE: 20 μM/l; Sigma), oxidized low-density lipoprotein (Ox-LDL) staining (1:50; Abcam),[18] myocardial protein expression of the lectin-like oxidized low-density lipoprotein receptor-1 (LOX-1; Cat# ab60178; Abcam), and the NADPH oxidase subunits gp91(Millipore; Cat# 07-024) and p67 (Cell Signaling; Cat# sc-15342). Myocardial apoptosis was assessed in LV sections double-stained with terminal deoxynucleotidyl transferase-mediated dUTP nick end end-labeling (TUNEL; Promega, Madison, WI, USA) and connexin-43 fluorescent staining, and caspase-3 (both 1:200; Santa Cruz Biotechnology, Inc.) fluorescent staining.[18] The number of TUNEL+ and caspase-3+ cells was quantified and averaged in each group. Myocardial expression of caspase-3 (Abcam; Cat# ab 52181), the apoptosis regulator protein B-cell lymphoma (Bcl)-2-associated-X protein (Bax) (Santa Cruz; 1:200) and Bcl-2 (Abcam; Cat# ab 53348) was measured by western blotting and Bax/Bcl-2 ratio calculated. Myocardial expression of the mitogen-activated protein kinases (MAPK) phosphorylated extracellular signal-regulated kinases (ERK)1/2 and p38 was also assessed by western blot (Cell Signaling; 1:1000, Cat# 4695 and Cat# 9211, respectively).

2.6 Effect of ELAM in healthy animals

For comparison, myocardial desmin and tubulin expression, cardiolipin content, synthesis, remodeling, and species profile, as well as mitochondria–SR interaction, were also assessed in six additional lean pigs treated with ELAM.

2.7 Statistical methods

Data are presented as median (range). Comparisons within and among the groups were performed using non-parametric Kruskal–Wallis followed by Dunn's comparison. A $P \leq 0.05$ was considered statistically significant. Statistical analysis was performed using JMP 10.0 software package (SAS Institute, Cary, NC, USA).

3. Results

3.1 Systemic characteristics and cardiac function

After 16 weeks of MetS or standard diet, body weight, mean blood pressure, and lipid fractions were higher in MetS compared with lean pigs (*Table 1*). Fasting glucose was similar among the groups, yet fasting insulin and HOMA-IR levels were elevated in MetS.

Heart rate was higher in MetS compared with lean pigs, whereas ejection fraction did not differ among the groups. LVMM tended to be higher in MetS compared with lean ($P = 0.06$). RPP was higher in MetS pigs, implying increased cardiac demand.

3.2 MetS alters mitochondrial organization and structure

Myocardial expression of TOM-20 was similar among the groups, suggesting preserved the myocyte content of mitochondria (see Supplementary material online, *Figure S1A*). Electron microscopy revealed that MetS mitochondria exhibited clustering, loss of linear registry, and disassociation with sarcomeres, thereby increasing intracellular space (*Figure 1B*). The number of subsarcolemal mitochondria was considerably lower in MetS compared to lean (*Figure 2A* and *B*). Contrarily, myocardial mitochondrial area and matrix density were preserved (*Figure 2C*). Myocardial expression of CRLS-1 remained unaltered (see Supplementary material online, *Figure S1B*), suggesting preserved cardiolipin synthesis. Although total cardiolipin content was comparable between lean and MetS (see Supplementary material online, *Figure S1C*), MetS decreased content of the tetra-linoleoyl cardiolipin (C18: 2)4 (*Figure 3A*), its most prominent species in the pig myocardium.[7] Contrarily, MetS increased more unsaturated cardiolipin species, including (C18:2)3(C18:1), (C18:2)2(C18:1)2, (C18:2)3(C20:3), (C18:2)3(C20:4), and (C18:2)3(C16:1), which are highly predisposed for oxidization. Myocardial expression of Taz-1 and ALCAT-1 mRNA was higher in MetS compared with lean pigs (*Figure 3B*).

In isolated myocardial mitochondria, ATP levels were comparable in lean and MetS pigs, yet ADP levels were higher in MetS (*Figure 4A*), so that ATP/ADP ratio decreased in MetS. Despite unchanged expression of all COX subunits (see Supplementary material online, *Figure S2*), COX-IV activity decreased in MetS compared to lean (*Figure 4B*).

H_2O_2 production increased in MetS vs. lean (*Figure 4C*). Expression of SOD-1 and SOD-2 decreased in MetS compared to lean (see Supplementary material online, *Figure S3*) and GSH/GSSG and NADPH/NADP ratio were significantly reduced (*Figure 4D*), whereas expression of TRX-2 and PRX-3 did not differ among the groups (see Supplementary material online, *Figure S3*).

Myocardial expression of MFN-1, OPA-1, MFF, and DRP-1 did not differ among the groups (see Supplementary material online, *Figure S4*), whereas expression of p62 was higher in MetS compared to lean (see Supplementary material online, *Figure S5A*). Furthermore, parkin expression and its co-localization with PINK-1 (M1 overlap coefficient) decreased in MetS (see Supplementary material online, *Figure S5B*), implying decreased mitophagy.

3.3 MetS impairs cytoskeletal–mitochondria–SR coupling

Immunofluorescence staining revealed that connexin-43 expression was unchanged, yet MetS decreased desmin and β2 tubulin immunoreactivity (*Figure 5A*). Contrarily, overall desmin and β2 tubulin protein expression did not differ among the groups (*Figure 5B*).

Total VDAC and RYR fluorescence did not differ among the groups, yet their overlap coefficient (M1) decreased in MetS (*Figure 6A*), suggesting impaired mitochondria–SR coupling. Colocalization between VDAC and TOM-20 as well as between RYR and SERCA-2a was almost complete (overlap coefficients ~1), confirming specific staining for mitochondria and SR, respectively (see Supplementary material online, *Figure S6*). Myocardial mitochondrial expression of MCU, the primary pathway for

Table 1 Systemic characteristics and cardiac function [median (range)] in study groups ($n = 6$ each) at 16 weeks

Parameter	Lean	MetS	MetS + ELAM	Dunn's comparison		
				Lean vs. MetS	Lean vs. MetS + ELAM	MetS vs. MetS + ELAM
Body weight (Kg)	73.5 (56.0–86.0)	92.0 (89.0–94.0)*	90.5 (85.0–97.0)*	0.011	0.022	NS
Serum creatinine (mg/dl)	1.6 (1.4–1.7)	1.5 (1.2–1.8)	1.5 (1.2–1.9)	NS	NS	NS
Fasting glucose (mg/dl)	122.5 (86.0–171.0)	116.0 (91.0–138.0)	115.0 (71.0–152.0)	NS	NS	NS
Fasting insulin (μU/ml)	0.2 (0.1–0.3)	0.4 (0.3–0.6)*	0.5 (0.3–0.7)*	0.013	0.025	NS
HOMA-IR score	0.6 (0.5–0.7)	1.9 (1.1–2.0)*	1.9 (1.7–2.1)*	0.007	0.019	NS
Plasma rennin activity (ng/ml/h)	0.2 (0.1–0.2)	0.15 (0.1–0.2)	0.2 (0.1–0.2)	NS	NS	NS
Total cholesterol (mg/dl)	82.5 (73.0–92.0)	486.0 (328.0–554.0)*	415.5 (219.0–677.0)*	0.011	0.015	NS
HDL cholesterol (mg/dl)	47.0 (41.0–57.0)	130.0 (101.0–180.0)*	105.0 (95.0–174.0)*	0.004	0.033	NS
LDL cholesterol (mg/dl)	33.8 (25.2–41.0)	369.7 (174.4–560.2)*	286.4 (229.4–544.0)*	0.012	0.012	NS
Triglycerides (mg/dl)	6.5 (5.0–9.0)	14.0 (12.0–33.0)*	16.5 (12.0–21.0)*	0.006	0.026	NS
Mean blood pressure (mmHg)	94.2 (80.3–104.7)	128.2 (113.7–133.7)*	122.9 (117.7–140.6)*	0.006	0.024	NS
Heart rate (beats/min)	73.3 (70.2–76.4)	84.5 (82.0–87.0)*	86.0 (81.0-89.0)*	0.006	0.024	NS
RPP (mmHg x beats/min)	7946.7 (6764.7–9826.4)	12463.6 (9793.8–13129.1)*	12117.1 (9430.3–12339.0)*	0.012	0.052	NS
Ejection fraction (%)	55.7 (50.8–59.6)	47.8 (46.0–63.7)	58.2 (52.0–70.2)	NS	NS	NS
LVMM(g)	133.0 (102.6–168.5)	152.9 (146.6–179.7)	156.8 (111.3–188.9)	NS	NS	NS

HOMA-IR: Homeostasis model assessment of insulin resistance; HDL: High-density lipoprotein; LDL: Low-density lipoprotein; LVMM: Left ventricular muscle mass; NS: Not significant.
*$P \leq 0.05$ vs. lean.

calcium entry into the mitochondrial matrix,[19] decreased in MetS compared to lean (*Figure 6B*), indicating impaired mitochondrial calcium handling.

3.4 MetS induces myocardial oxidative stress and apoptosis

Myocardial fat deposition, expression of Ox-LDL, and superoxide anion production were all higher in MetS compared to lean (*Figure 7A*). LOX-1 was up-regulated in MetS, as were myocardial expression of gp91 and p67 (see Supplementary material online, *Figure S7*).

The number of TUNEL and caspase-3 positive cells was elevated in the MetS (*Figure 7B*). TUNEL-positive staining co-localized with connexin-43, suggesting apoptotic cardiomyocytes. Myocardial expression of caspase-3 (*Figure 7C*) was higher in MetS compared to lean. Despite some biological variability (denoted by the last two MetS + ELAM samples), caspase-3 expression reached statistical significance. Myocardial expression of Bax was also higher in MetS compared to lean, whereas Bcl-2 was down-regulated. Consequently, Bax/Bcl-2 ratio was higher in MetS (see Supplementary material online, *Figure S8*). Myocardial expression of both phosphorylated ERK1/2 and p38 increased in MetS compared to lean (see Supplementary material online, *Figure S9*).

3.5 Mitoprotection preserves the cytoskeletal-mitochondria-SR complex

Treatment with ELAM restored the typical linear registry of cardiomyocyte mitochondria of one or two mitochondria per sarcomere (*Figure 1B*) and increased the number of subsarcolemal mitochondria (*Figure 2A and B*). ELAM administration also increased (18:2)4 cardiolipin content and decreased the content of species prone to oxidization, such as (C18:2)3(C18:1), (C18:2)2(C:18:1)2, and (C18:2)3(C20:3) (*Figure 3A*). Although Taz-1 expression remained up-regulated, ELAM normalized expression of ALCAT-1 (*Figure 3B*), a major regulator of abnormal cardiolipin remodeling.[20]

ELAM also normalized mitochondrial ADP levels and ATP/ADP ratio (*Figure 4A*) and COX-IV activity (*Figure 4B*), despite preserved COX-I, II, III, and IV expression (see Supplementary material online. *Figure S2*). Mitochondrial production of H_2O_2 decreased (*Figure 4C*), whereas expression of SOD-1 and SOD-2 remained unchanged in ELAM-treated pigs (see Supplementary material online, *Figure S3*). However, GSH/GSSG and NADPH/NADP ratio, decreased in MetS, normalized in MetS + ELAM pigs (*Figure 4D*), suggesting restoration of mitochondrial antioxidant defenses. Furthermore, mitoprotection improved mitophagy (see Supplementary material online, *Figure S5*), desmin and β2 tubulin immunoreactivity (*Figure 5*), increased the overlap coefficient of VDAC and RYR fluorescence (*Figure 6A*), and MCU expression (*Figure 6B*), suggesting preserved mitochondrial and SR juxtaposition and calcium handling.

3.6 ELAM attenuates MetS-induced myocardial changes

Mitoprotection attenuated myocardial expression of LOX-1, p67 (see Supplementary material online, *Figure S7*), and Ox-LDL, and superoxide anion production (*Figure 7A*). Finally, ELAM decreased the number of TUNEL and caspase-3 positive cells (*Figure 7B*), myocardial caspase-3 (*Figure 7C*), Bax/Bcl-2 ratio (see Supplementary material online, *Figure S9*), as well as phosphorylated ERK1/2 and p38 expression (see Supplementary material online, *Figure S10*).

3.7 ELAM does not affect cardiac structure and function in healthy animals

Myocardial desmin and tubulin expression, total cardiolipin content, synthesis, remodeling, and species profile (see Supplementary material

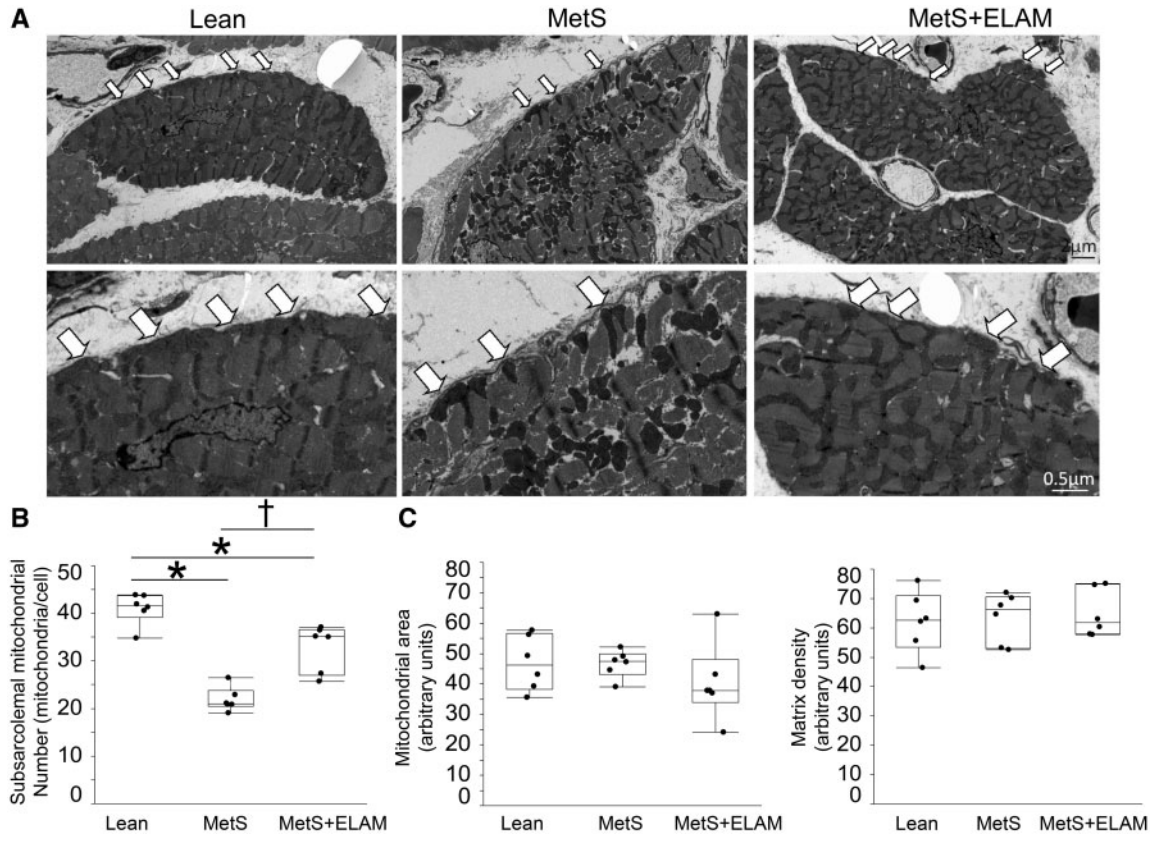

Figure 2 *Mitoprotection restored subsarcolemal mitochondrial density.* (*A*) Representative transmission electron microscopy images of cross-sectioned cardiomyocytes showing distribution of mitochondria. (*B*) The number of subsarcolemal mitochondria (arrows) was lower in MetS compared to Lean, but increased in MetS + ELAM ($n = 6$/group). (*C*) Mitochondrial area and matrix density did not differ among the groups ($n = 6$/group). $^{*}P < 0.05$ vs. lean, $^{\dagger}P < 0.05$ vs. MetS + ELAM.

online, *Figure S11*), as well as mitochondria–SR interaction (see Supplementary material online, *Figure S12*) were similar in lean and lean + ELAM pigs.

4. Discussion

The current study shows that cardiac abnormalities at the early stages of MetS are characterized by cardiomyocyte mitochondrial disorganization and altered cytoskeletal–mitochondria–SR interaction, inducing myocardial oxidative stress and apoptosis, despite preserved cardiac function. Notably, mitoprotection with ELAM improved these reversible changes, implicating mitochondrial damage in cardiac injury in experimental MetS, and suggesting novel therapeutic targets for preserving the myocardium in early MetS.

MetS is considered a global epidemic and a major public health problem, being an independent risk factor for cardiovascular disease.[1,2] Long-term MetS induces cardiac remodeling and dysfunction, but the initial underlying mechanisms remain elusive.

In the current study, we used a novel swine model of MetS that we recently developed to pinpoint the mechanisms responsible for MetS-associated cardiac damage.[11] Human MetS is defined by the presence of at least three of the following: obesity, hypertension, high triglyceride levels, reduced HDL levels, and elevated fasting glucose levels or insulin resistance.[21] After 16 weeks of diet, our MetS pigs developed obesity and hypertriglyceridemia, hypertension and insulin resistance, confirming development of MetS, yet glucose levels remained unaltered, underscoring its early pre-diabetes stage. HDL levels were elevated possibly due to decreased cholesteryl ester transfer protein activity,[22,23] whereas cardiac function remained unaltered, consistent with findings in adolescent patients with MetS.[24] Nontheless, disorganization of the cardiomyocyte cytoskeletal-mitochondria-SR network could already be detected, associated with myocardial oxidative stress and apoptosis. Importantly, longitudinal studies have shown that subtle impairments in the early stage of MetS may later precipitate and promote cardiac dysfunction.[25,26]

Cardiac mitochondria not only provide most of the ATP necessary for cardiac function but also regulate cardiomyocyte calcium homeostasis, redox balance, and cell fate.[27] To ensure adequate function, myocardial mitochondria are intimately associated with myofibrils, where the cytoskeleton functions as a linkage coordinator. Desmin forms connections between Z disks and mitochondria that maintain cardiomyocyte shape and mechanochemical signaling. Likewise, β2 tubulin is involved in interactions between the mitochondria and cytoskeleton and controls the permeability of the outer mitochondrial membrane protein VDAC to ADP and ATP, sustaining mitochondrial and cellular physiology.[28] The importance of mitochondrial organization is underscored by the observation that hearts from rats with volume overload show

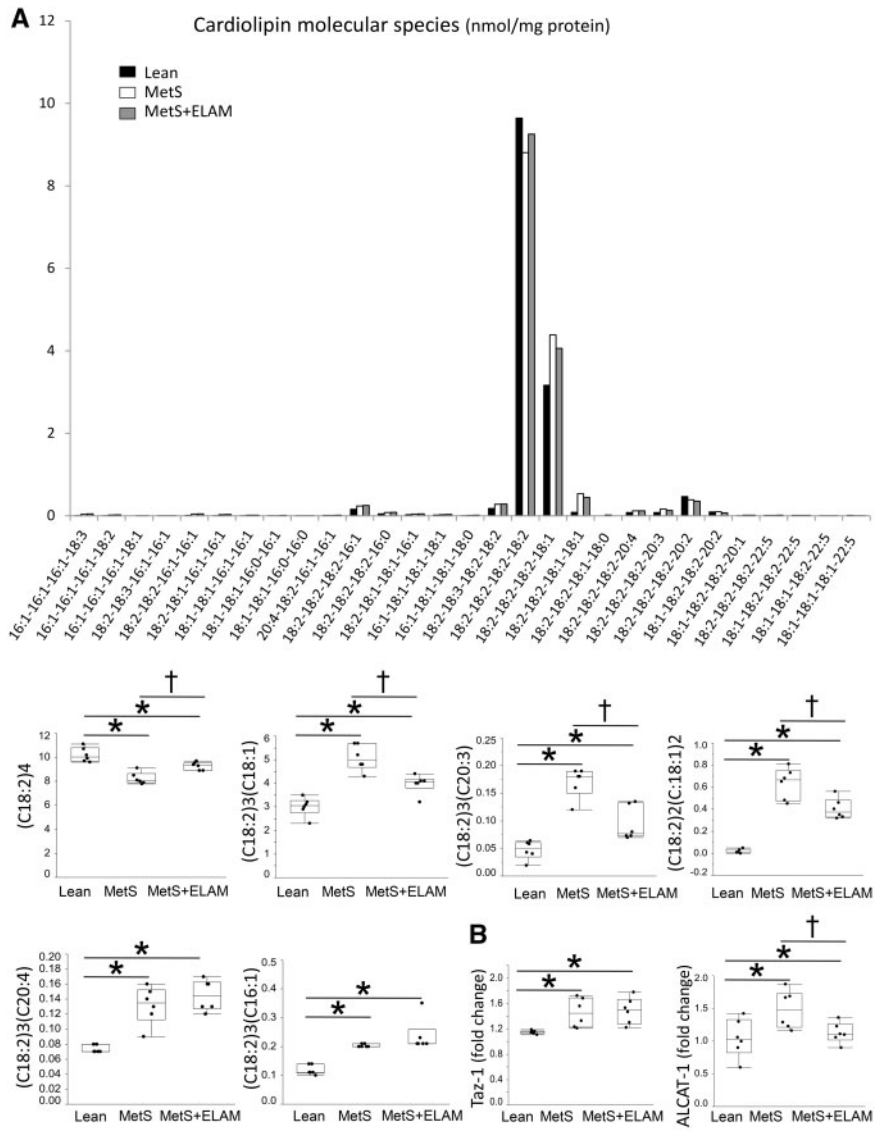

Figure 3 *MetS altered cardiolipin species profile.* (*A*) Myocardial levels of tetralinoleoyl (C18:2)4 cardiolipin decreased in MetS, whereas content of species rich in linoleic (C18:2)3(C18:1) and (C18:2)2(C:18:1)2, eicostrienoic (C18:2)3(C20:3), arachidonic (C18:2)3(C20:4), and palmitoleic (C18:2)3(C16:1) acids increased in MetS compared to lean. Treatment with ELAM restored (18:2)4 cardiolipin content and decreased the content of species prone to oxidization, such as (C18:2)3(C18:1), (C18:2)2(C:18:1)2, and (C18:2)3(C20:3) ($n = 6$/group). (*B*) mRNA expression of the cardiolipin regulators tafazzin (Taz)-1 and acyl-CoA: lysocardiolipin acyltransferase (ALCAT)-1 ($n = 6$/group). *$P < 0.05$ vs. lean, †$P < 0.05$ vs. MetS + ELAM.

mitochondrial-cytoskeletal abnormalities, associated with myocardial oxidative stress, and LV dysfunction.[8]

In this study, we found that early MetS induced loss of mitochondrial linear arrangement, reflected by increased intracellular space and mitochondrial clustering, which was paralleled by decreased myocardial desmin and β2 tubulin immunoreactivity. However, the unaltered total expression of these proteins implies that this resulted from changes in protein alignment of quaternary structure, which might have interfered with their binding properties. In agreement, studies in failing right ventricles have shown decreased myocardial immunoreactivity of cytoskeletal proteins despite unaltered total protein expression, suggesting dissociation from the contractile apparatus and cytoplasmic redistribution.[29] These changes may be evoked by increased myocardial expression of caspase-3, which phosphorylates specific residues in desmin, altering its distribution within the cell.[30,31] Additionally, MetS-induced alterations in cellular redox status may induce mitochondrial damage[8] and disrupt the organization of microtubules, favoring their depolymerization.[32] In line with this contention, we found that mitochondrial H_2O_2 production was increased, whereas antioxidant defenses (GSH/GSSG and NADPH/NADP) were blunted in MetS pigs, suggesting impaired redox balance. MetS also decreased the number of subsarcolemmal mitochondria, which provide energy for electrolyte and protein transport across the sarcolemma, suggesting redistribution of mitochondria.

Interestingly, MetS-induced changes in myocardial profiles of cardiolipin, an inner mitochondrial membrane phospholipid that regulates mitochondrial energy production[33] and prevents mPTP opening, averting the

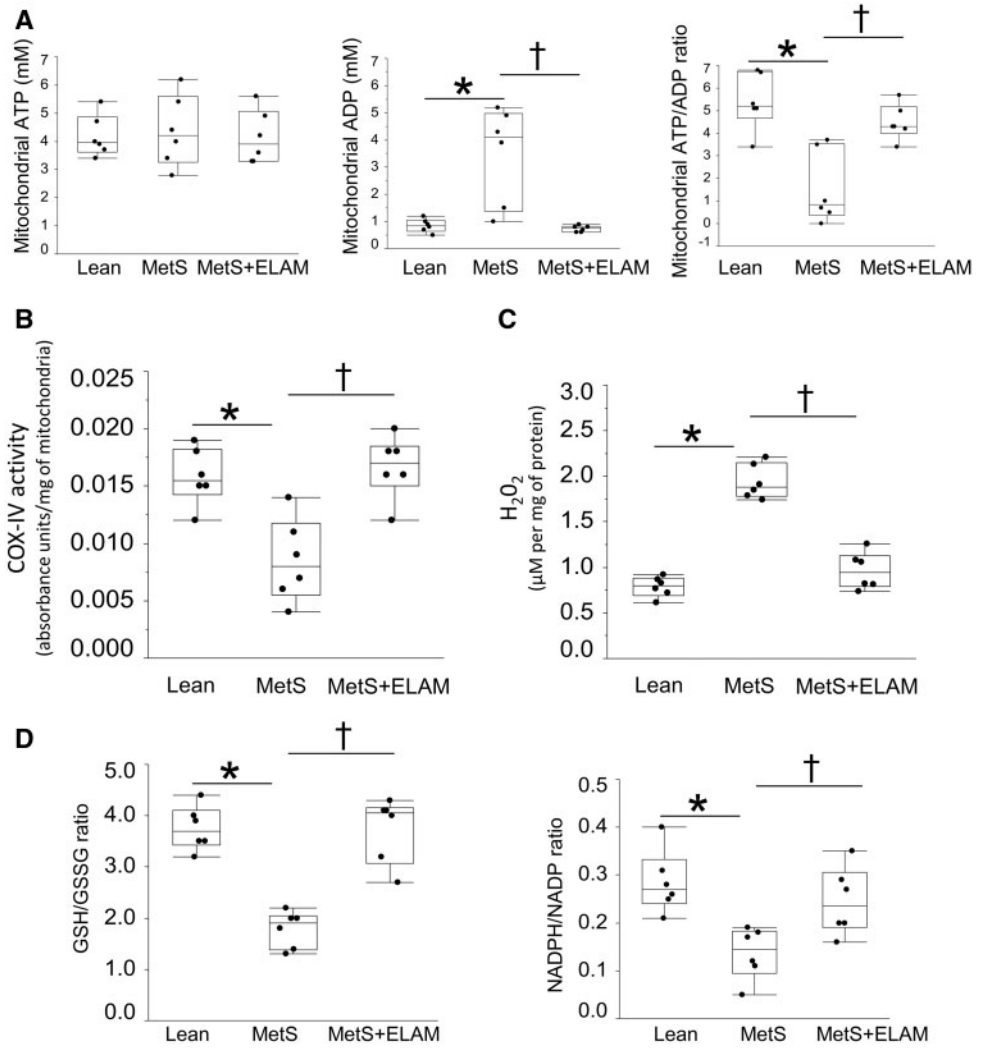

Figure 4 *ELAM improved mitochondrial function Dand redox balance.* (*A*) In isolated myocardial mitochondria, ATP levels were comparable in all groups, yet ADP levels were higher in MetS and normalized in MetS + ELAM, as was ATP/ADP ratio ($n = 6$/group). (*B*) COX-IV activity decreased in MetS compared to lean, but normalized in ELAM-treated pigs. (*C*) H_2O_2 production increased in MetS but normalized in MetS + ELAM. (*D*) GSH/GSSG and NADPH/NADP ratio decreased in MetS, but normalized in ELAM-treated pigs ($n = 6$/group). *$P < 0.05$ vs. lean, †$P < 0.05$ vs. MetS + ELAM .

release of cytochrome-c to the cytoplasm and the initiation of apoptosis.[34] Furthermore, cardiolipin promotes the uptake of GSH from the cytoplasm[35] and the formation and interaction of respiratory supercomplexes and the ADP/ATP carrier,[36] regulating mitochondrial organization, internal milieu, and function.[33] However, cardiolipin is sensitive to oxidative damage, due to its high content of polyunsaturated fatty acid and its location near the site of ROS production. Susceptibility for oxidation increases when cardiolipin is enriched with unsaturated fatty acids. In this study, we found that MetS decreased myocardial content of the polyunsaturated tetralinoleoyl (C18:2)4 cardiolipin, but increased monounsaturated species, which are highly predisposed to oxidation.[37] MetS also increased both normal and abnormal cardiolipin remodeling, reflected in upregulated mRNA expression of Taz-1 and ALCAT-1, which was associated with decreased COX-IV activity and mitochondrial ATP/ADP imbalance, possibly due to altered assembly of the electron transport chain complexes and/or interaction with the ADP/ATP carrier. MetS also impaired mitophagy, reflected in decreased parkin/PINK-1 colocalization and increased expression of p62, in line with recent findings of decreased mitophagy in cardiolipin-deficient cells.[38] Importantly, MetS-induced failure to remove defective, ROS-producing mitochondria, might have exacerbated oxidative damage.

Cardiac mitochondria are adjacent to the calcium release sites of the SR and facilitate calcium and ADP exchange between the SR RyR and mitochondrial VDAC channel.[39] Calcium uptake activates the TCA cycle enzymes, stimulating ATP production.[40] Moreover, mitochondrial calcium induces NADPH regeneration, increasing antioxidant activity.[5] Therefore, MetS-induced interruption of SR-mitochondria communication may have impaired calcium exchange and triggered oxidative stress and inefficient energy production, as we have shown in swine renovascular hypertension.[7] Furthermore, MetS down-regulated MCU, an anion channel protein that mediates mitochondrial calcium uptake.[19] Therefore, MetS-induced SR-mitochondria dissociation and impaired mitochondrial

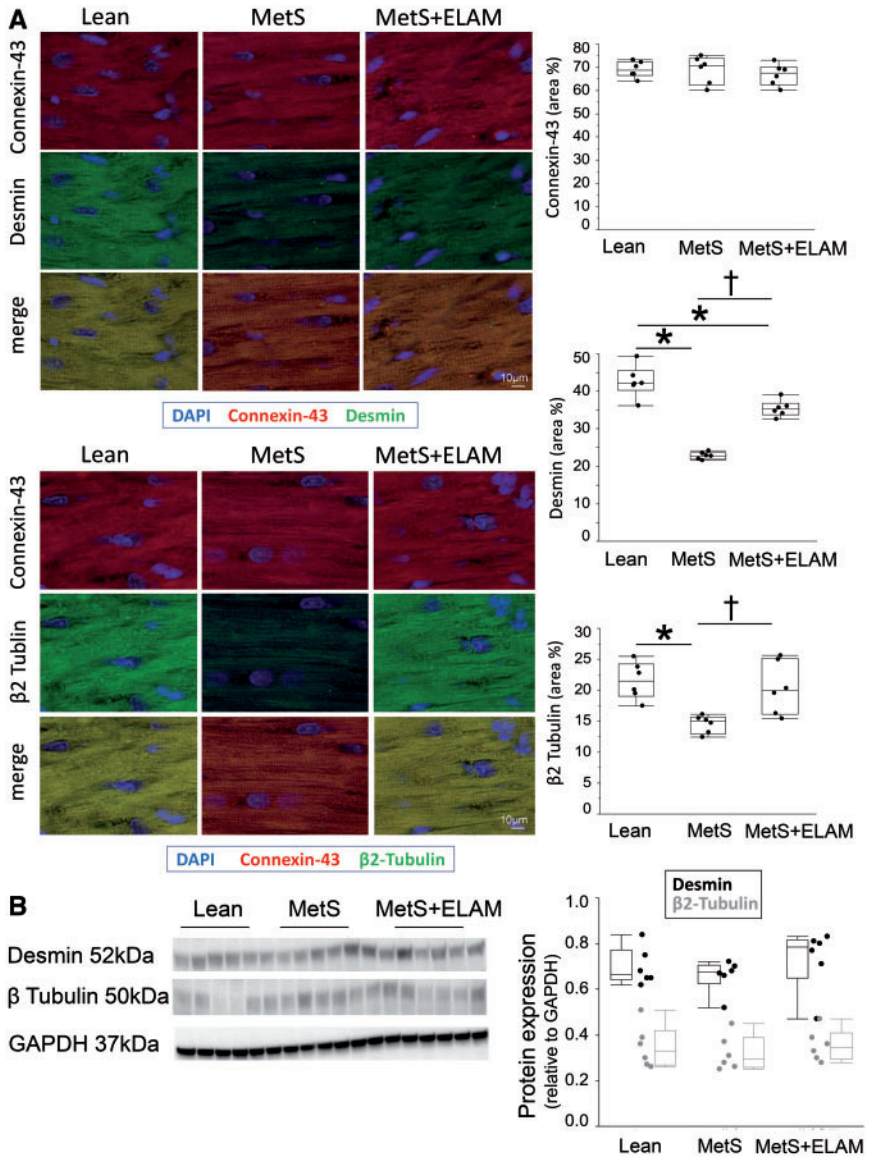

Figure 5 *MetS caused cardiomyocyte cytoskeletal abnormalities.* (*A*) Myocardial double immunofluorescence staining of connexin-43 (red)/desmin (green) and connexin-43 (red)/β2 tubulin (red), and their quantification ($n = 6$/group). (*B*) Desmin and β2 tubulin protein expression did not differ among the groups ($n = 6$/group) .

antioxidant defenses and calcium handling might precede development of measurable cardiac dysfunction in this model.

In addition, MetS increased extracellular (Ox-LDL) and myocardial (superoxide) oxidative stress, activating LOX signaling and NADPH.[41] This in turn might have induced apoptosis via MAPK signaling, particularly p38 and ERK1/2,[42] aggravating mitochondrial damage and creating a negative cycle of mitochondrial dysfunction, oxidative stress, and apoptosis. Congruently, myocardial apoptosis observed in the early stages of experimental MetS is an important contributor to progression to cardiac dysfunction.[43–45] Furthermore, this is consistent with our and other previous studies in swine that showed slightly increased myocardial apoptosis, which was magnified upon transition to MetS.[44,45]

The mechanism by which MetS damaged the swine cardiac mitochondria may be multifactorial, including dyslipidemia,[46] activation of mitochondrial angiotensin-II receptors,[47] insulin resistance,[48] and increased metabolic workload, reflected in elevated RPP (see Supplementary material online, *Figure S10*). Interaction among these factors may collaboratively contribute to cardiac mitochondrial damage.

To establish the role of mitochondrial abnormalities in MetS-induced cardiac damage, we treated MetS pigs with a unique mitochondria-targeted peptide, which concentrates in the organelle and exerts important antioxidant effects. ELAM binds selectively to and stabilizes cardiolipin, protecting mitochondrial cristae structure and organization.[49] In addition, ELAM improves mitochondrial bioenergetics, inhibits the activity of cytochrome-c peroxidase and mPTP opening, preventing apoptosis

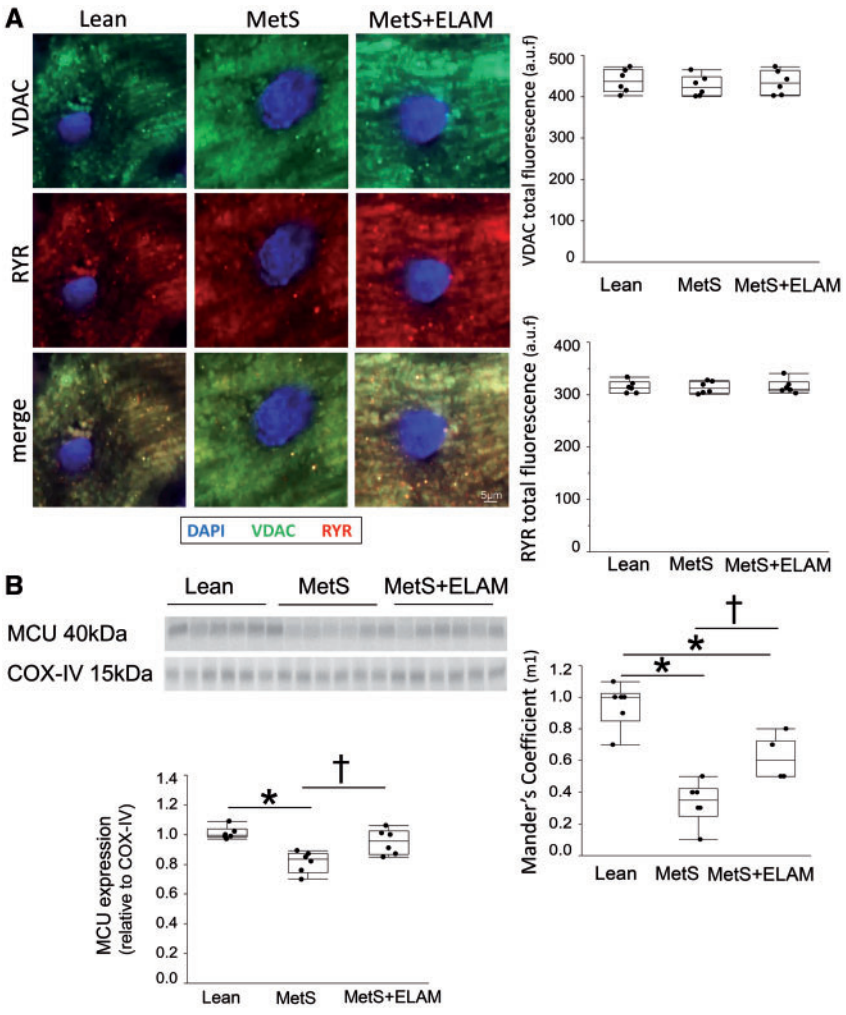

Figure 6 *MetS altered mitochondria-sarcoplasmic reticulum interaction.* (*A*) Representative myocardial double immunofluorescence staining of the mitochondrial voltage-dependent anion channel (VDAC) and the sarcoplasmic-reticulum marker ryanodine receptor (RYR). Although total VDAC and RYR fluorescence did not differ among the groups, their overlap coefficient (M1) decreased in MetS, but improved in MetS + ELAM ($n = 6$/group). (*B*) Myocardial expression of MCU decreased in MetS, but was restored in MetS + ELAM ($n = 6$/group). *$P < 0.05$ vs. lean, †$P < 0.05$ vs. MetS + ELAM.

and oxidative stress.[33] Consequently, ELAM attenuates experimental myocardial ischemia-reperfusion injury and hypertensive cardiomyopathy.[7,18,50,51] The current study extends those observations and demonstrates that ELAM also improves mitochondrial organization and function, and cytoskeletal–mitochondrial–SR interaction in early MetS, possibly by decreasing myocardial apoptosis and oxidative stress. Given that our model develops MetS after 12 weeks of diet[11] and that mitochondrial dysfunction continues developing to week 16,[44] its effects were likely both preventive and restorative. Importantly, ELAM did not affect cardiac structure and function in healthy animals, supporting our previous observations in swine.[7,52,53] Therefore, our study implicates mitochondrial reversible changes in MetS-induced cardiac damage, and position the mitochondrion as an important therapeutic target.

Our study is limited by the use of young animals and the relatively short duration of the disease. Yet, swine myocardial anatomy and physiology are similar to humans, and our model replicates many features of human MetS. Given the variability in some of the results and the small number of animals, these observations need to be interpreted with caution and confirmed in larger studies. Myocardial damage in our model is subtle, and mostly reversible, corresponding to the early stage of MetS. Our study cannot establish a definitive cause-effect relationship between mitochondrial damage and cytoskeletal abnormalities in experimental MetS, yet mitoprotection was sufficient to confer potent protective effects and restore myocardial mitochondrial organization, linking mitochondrial damage and cardiomyocyte cytoskeletal and SR abnormalities in swine MetS. Nevertheless, a longer observation period may be needed to achieve greater impairments in cardiac structure and function in MetS pigs.

In summary, this study shows that prior to any measurable changes in cardiac function, MetS induces in myocardial mitochondria reversible changes, characterized by disorganized cytoskeletal–mitochondrial–SR architecture, associated with myocardial oxidative stress and apoptosis. Treatment with ELAM preserved the cardiomyocyte cytoskeletal-mitochondrial-SR network, and attenuated myocardial oxidative stress and apoptosis, underscoring the cardioprotective properties of

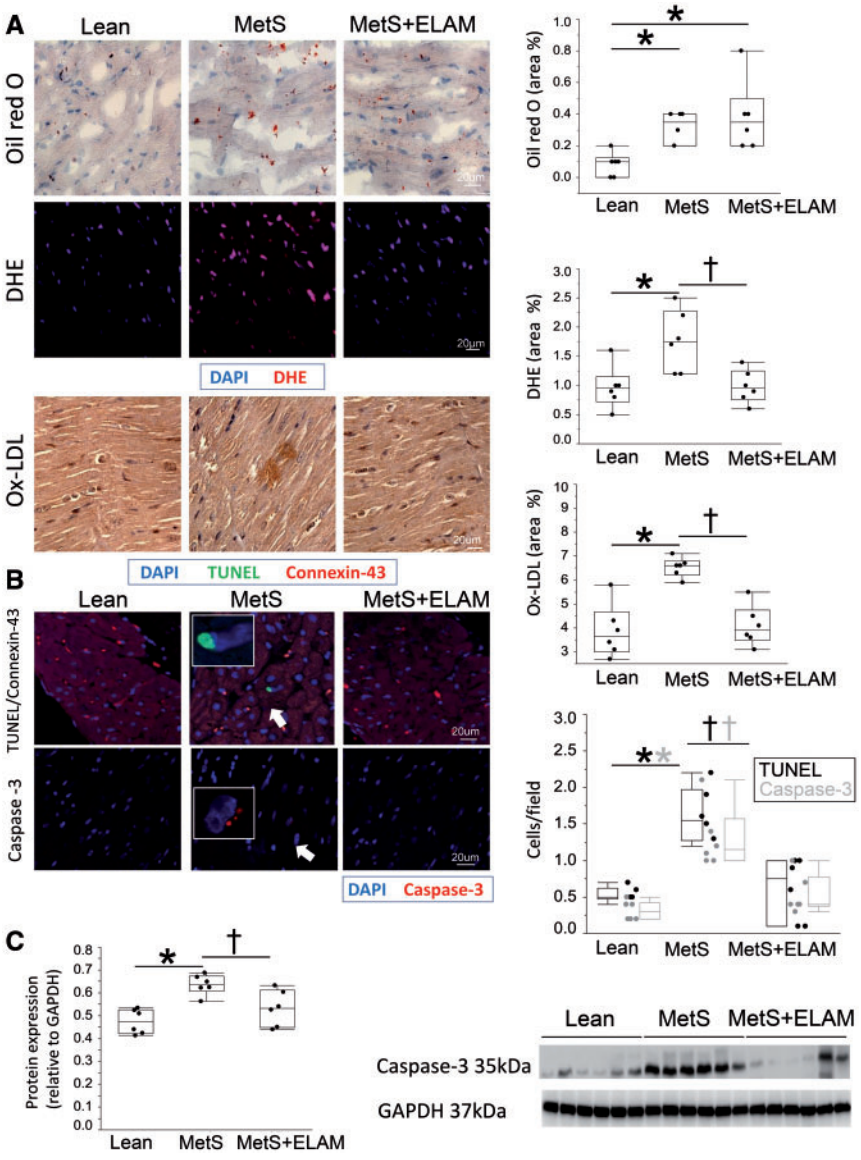

Figure 7 *Mitoprotection attenuated cardiomyocyte apoptosis and oxidative stress.* (*A*) Representative myocardial Oil-red-O, dihydroethidium, and Ox-LDL staining, and quantification of intra-cardiac fat deposition, production of superoxide anion, and Ox-LDL immunoreactivity ($n = 6$/group). (*B*) The number of terminal deoxynucleotidyl transferase dUTP nick end labeling (TUNEL, green) and caspase-3 (red) apoptotic cells was higher in MetS compared to Lean, but normalized in MetS + ELAM ($n = 6$/group). Red: connexin-43. (*C*) Myocardial expression of caspase-3 increased in MetS compared to lean, but normalized in ELAM-treated pigs ($n = 6$/group). *$P < 0.05$ vs. lean, †$P < 0.05$ vs. MetS + ELAM.

mitoprotection in early MetS. Further studies are required to confirm the efficacy of this approach for cardiac protection in MetS.

Supplementary material

Supplementary material is available at *Cardiovascular Research* online.

Conflict of interest: none declared.

Funding

This work was supported by research grants from Stealth BioTherapeutics, Inc., and from the National Institutes of Health (DK106427, DK73608, DK104273, HL123160, and DK102325).

References

1. O'Neill S, O'driscoll L. Metabolic syndrome: a closer look at the growing epidemic and its associated pathologies. *Obes Rev* 2015;**16**:1–12.
2. Perrone-Filardi P, Paolillo S, Costanzo P, Savarese G, Trimarco B, Bonow RO. The role of metabolic syndrome in heart failure. *Eur Heart J* 2015;**36**:2630–2634.
3. Sequeira V, Nijenkamp LL, Regan JA, van der Velden J. The physiological role of cardiac cytoskeleton and its alterations in heart failure. *Biochim Biophys Acta* 2014;**1838**:700–722.
4. Rostovtseva TK, Sheldon KL, Hassanzadeh E, Monge C, Saks V, Bezrukov SM, Sackett DL. Tubulin binding blocks mitochondrial voltage-dependent anion channel and regulates respiration. *Proc Natl Acad Sci Usa U.S.A*2008;**105**:18746–18751.
5. Fernandez-Sanz C, Ruiz-Meana M, Miro-Casas E, Nuñez E, Castellano J, Loureiro M, Barba I, Poncelas M, Rodriguez-Sinovas A, Vázquez J, Garcia-Dorado D. Defective sarcoplasmic reticulum-mitochondria calcium exchange in aged mouse myocardium. *Cell Death Dis* 2014;**5**:e1573.
6. Eirin A, Lerman A, Lerman LO. Mitochondrial injury and dysfunction in hypertension-induced cardiac damage. *Eur Heart J* 2014;**35**:3258–3266.

7. Eirin A, Ebrahimi B, Kwon SH, Fiala JA, Williams BJ, Woollard JR, He Q, Gupta RC, Sabbah HN, Prakash YS, Textor SC, Lerman A, Lerman LO. Restoration of mitochondrial cardiolipin attenuates cardiac damage in swine renovascular hypertension. *J Am Heart Assoc* 2016;**5**:e003118.
8. Yancey DM, Guichard JL, Ahmed MI, Zhou L, Murphy MP, Johnson MS, Benavides GA, Collawn J, Darley-Usmar V, Dell'italia LJ. Cardiomyocyte mitochondrial oxidative stress and cytoskeletal breakdown in the heart with a primary volume overload. *Am J Physiol Heart Circ Physiol* 2015;**308**:H651–H663.
9. Dong F, Li Q, Sreejayan N, Nunn JM, Ren J. Metallothionein prevents high-fat diet induced cardiac contractile dysfunction: role of peroxisome proliferator activated receptor gamma coactivator 1alpha and mitochondrial biogenesis. *Diabetes* 2007;**56**: 2201–2212.
10. Boudina S, Sena S, Theobald H, Sheng X, Wright JJ, Hu XX, Aziz S, Johnson JI, Bugger H, Zaha VG, Abel ED. Mitochondrial energetics in the heart in obesity-related diabetes: direct evidence for increased uncoupled respiration and activation of uncoupling proteins. *Diabetes* 2007;**56**:2457–2466.
11. Pawar AS, Zhu XY, Eirin A, Tang H, Jordan KL, Woollard JR, Lerman A, Lerman LO. Adipose tissue remodeling in a novel domestic porcine model of diet-induced obesity. *Obesity (Silver Spring)* 2015;**23**:399–407.
12. Eirin A, Ebrahimi B, Zhang X, Zhu XY, Woollard JR, He Q, Textor SC, Lerman A, Lerman LO. Mitochondrial protection restores renal function in swine atherosclerotic renovascular disease. *Cardiovasc Res* 2014;**103**:461–472.
13. Eirin A, Li Z, Zhang X, Krier JD, Woollard JR, Zhu XY, Tang H, Herrmann SM, Lerman A, Textor SC, Lerman LO. A mitochondrial permeability transition pore inhibitor improves renal outcomes after revascularization in experimental atherosclerotic renal artery stenosis. *Hypertension* 2012;**60**:1242–1249.
14. Eirin A, Zhu XY, Ferguson CM, Riester SM, van Wijnen AJ, Lerman A, Lerman LO. Intra-renal delivery of mesenchymal stem cells attenuates myocardial injury after reversal of hypertension in porcine renovascular disease. *Stem Cell Res Ther* 2015;**6**:7.
15. Zhang X, Li ZL, Crane JA, Jordan KL, Pawar AS, Textor SC, Lerman A, Lerman LO. Valsartan regulates myocardial autophagy and mitochondrial turnover in experimental hypertension. *Hypertension* 2014;**64**:87–93.
16. Chade AR, Rodriguez-Porcel M, Grande JP, Zhu X, Sica V, Napoli C, Sawamura T, Textor SC, Lerman A, Lerman LO. Mechanisms of renal structural alterations in combined hypercholesterolemia and renal artery stenosis. *Arterioscler Thromb Vasc Biol* 2003;**23**:1295–1301.
17. Pi J, Bai Y, Zhang Q, Wong V, Floering LM, Daniel K, Reece JM, Deeney JT, Andersen ME, Corkey BE, Collins S. Reactive oxygen species as a signal in glucose-stimulated insulin secretion. *Diabetes* 2007;**56**:1783–1791.
18. Eirin A, Williams BJ, Ebrahimi B, Zhang X, Crane JA, Lerman A, Textor SC, Lerman LO. Mitochondrial targeted peptides attenuate residual myocardial damage after reversal of experimental renovascular hypertension. *J Hypertens* 2014;**32**:154–165.
19. Baughman JM, Perocchi F, Girgis HS, Plovanich M, Belcher-Timme CA, Sancak Y, Bao XR, Strittmatter L, Goldberger O, Bogorad RL, Koteliansky V, Mootha VK. Integrative genomics identifies MCU as an essential component of the mitochondrial calcium uniporter. *Nature* 2011;**476**:341–345.
20. Li J, Romestaing C, Han X, Li Y, Hao X, Wu Y, Sun C, Liu X, Jefferson LS, Xiong J, Lanoue KF, Chang Z, Lynch CJ, Wang H, Shi Y. Cardiolipin remodeling by ALCAT1 links oxidative stress and mitochondrial dysfunction to obesity. *Cell Metab* 2010;**12**: 154–165.
21. Cameron AJ, Shaw JE, Zimmet PZ. The metabolic syndrome: prevalence in worldwide populations. *Endocrinol Metab Clin North Am* 2004;**33**:351–375. table of contents.
22. Barter PJ, Ha YC, Calvert GD. Studies of esterified cholesterol in sub-fractions of plasma high density lipoproteins. *Atherosclerosis* 1981;**38**:165–175.
23. Daugherty A, Tall AR, Daemen M, Falk E, Fisher EA, Garcia-Cardena G, Lusis AJ, Owens AP, 3rd, Rosenfeld ME, Virmani R. American Heart Association Council on Arteriosclerosis, Thrombosis and Vascular Biology; and Council on Basic Cardiovascular Sciences. Recommendation on design, execution, and reporting of animal atherosclerosis studies: a scientific statement from the American heart association. *Arterioscler Thromb Vasc Biol* 2017;**37**:e131–e157.
24. Rowland TW. Effect of obesity on cardiac function in children and adolescents: a review. *J Sports Sci Med* 2007;**6**:319–326.
25. Alpert MA. Obesity cardiomyopathy: pathophysiology and evolution of the clinical syndrome. *Am J Med Sci* 2001;**321**:225–236.
26. Wong CY, O'moore-Sullivan T, Leano R, Byrne N, Beller E, Marwick TH. Alterations of left ventricular myocardial characteristics associated with obesity. *Circulation* 2004; **110**:3081–3087.
27. Duchen MR. Mitochondria in health and disease: perspectives on a new mitochondrial biology. *Mol Aspects Med* 2004;**25**:365–451.
28. Varikmaa M, Bagur R, Kaambre T, Grichine A, Timohhina N, Tepp K, Shevchuk I, Chekulayev V, Metsis M, Boucher F, Saks V, Kuznetsov AV, Guzun R. Role of mitochondria-cytoskeleton interactions in respiration regulation and mitochondrial organization in striated muscles. *Biochim Biophys Acta* 2014;**1837**:232–245.
29. Lemler MS, Bies RD, Frid MG, Sastravaha A, Zisman LS, Bohlmeyer T, Gerdes AM, Reeves JT, Stenmark KR. Myocyte cytoskeletal disorganization and right heart failure in hypoxia-induced neonatal pulmonary hypertension. *Am J Physiol Heart Circ Physiol* 2000;**279**:H1365–H1376.
30. Costa ML, Escaleira R, Cataldo A, Oliveira F, Mermelstein CS. Desmin: molecular interactions and putative functions of the muscle intermediate filament protein. *Braz J Med Biol Res* 2004;**37**:1819–1830.
31. Huang F, Huang M, Zhou G, Xu X, Xue M. In vitro proteolysis of myofibrillar proteins from beef skeletal muscle by caspase-3 and caspase-6. *J Agric Food Chem* 2011; **59**:9658–9663.
32. Lee CF, Liu CY, Hsieh RH, Wei YH. Oxidative stress-induced depolymerization of microtubules and alteration of mitochondrial mass in human cells. *Ann N Y Acad Sci* 2005;**1042**:246–254.
33. Szeto HH. First-in-class cardiolipin-protective compound as a therapeutic agent to restore mitochondrial bioenergetics. *Br J Pharmacol* 2014;**171**:2029–2050.
34. Petrosillo G, Ruggiero FM, Paradies G. Role of reactive oxygen species and cardiolipin in the release of cytochrome c from mitochondria. *FASEB J* 2003;**17**:2202–2208.
35. Patil VA, Fox JL, Gohil VM, Winge DR, Greenberg ML. Loss of cardiolipin leads to perturbation of mitochondrial and cellular iron homeostasis. *J Biol Chem* 2013;**288**: 1696–1705.
36. Claypool SM, Oktay Y, Boontheung P, Loo JA, Koehler CM. Cardiolipin defines the interactome of the major ADP/ATP carrier protein of the mitochondrial inner membrane. *J Cell Biol* 2008;**182**:937–950.
37. Belikova NA, Vladimirov YA, Osipov AN, Kapralov AA, Tyurin VA, Potapovich MV, Basova LV, Peterson J, Kurnikov IV, Kagan VE. Peroxidase activity and structural transitions of cytochrome c bound to cardiolipin-containing membranes. *Biochemistry* 2006;**45**:4998–5009.
38. Shen Z, Li Y, Gasparski AN, Abeliovich H, Greenberg ML. Cardiolipin regulates mitophagy through the protein kinase C pathway. *J Biol Chem* 2017;**292**:2916–2923.
39. Kohlhaas M, Maack C. Adverse bioenergetic consequences of Na+-Ca2+ exchanger-mediated Ca2+ influx in cardiac myocytes. *Circulation* 2010;**122**:2273–2280.
40. Denton RM. Regulation of mitochondrial dehydrogenases by calcium ions. *Biochim Biophys Acta* 2009;**1787**:1309–1316.
41. Dong Q, Xiang R, Zhang DY, Qin S. Ox-LDL increases OX40L in endothelial cells through a LOX-1-dependent mechanism. *Braz J Med Biol Res* 2013;**46**:765–770.
42. Zhang K, Meng X, Kong J, Liu FF, Yang JM, Gao F, Zhang Y, Zhang C. Simvastatin increases Prolyl-4-Hydroxylase alpha1 expression in atherosclerotic plaque and ox-LDL-stimulated human aortic smooth muscle cells via p38 MAPK and ERK1/2 signaling. *J Mol Cell Cardiol* 2013;**65**:43–50.
43. Katare RG, Caporali A, Oikawa A, Meloni M, Emanueli C, Madeddu P. Vitamin B1 analog benfotiamine prevents diabetes-induced diastolic dysfunction and heart failure through Akt/Pim-1-mediated survival pathway. *Circ Heart Fail* 2010;**3**:294–305.
44. Li ZL, Woollard JR, Ebrahimi B, Crane JA, Jordan KL, Lerman A, Wang SM, Lerman LO. Transition from obesity to metabolic syndrome is associated with altered myocardial autophagy and apoptosis. *Arterioscler Thromb Vasc Biol* 2012;**32**:1132–1141.
45. Elmadhun NY, Sabe AA, Lassaletta AD, Chu LM, Kondra K, Sturek M, Sellke FW. Metabolic syndrome impairs notch signaling and promotes apoptosis in chronically ischemic myocardium. *J Thorac Cardiovasc Surg* 2014;**148**:1048–1055; discussion 1055.
46. Knight-Lozano CA, Young CG, Burow DL, Hu ZY, Uyeminami D, Pinkerton KE, Ischiropoulos H, Ballinger SW. Cigarette smoke exposure and hypercholesterolemia increase mitochondrial damage in cardiovascular tissues. *Circulation* 2002;**105**:849–854.
47. Doughan AK, Harrison DG, Dikalov SI. Molecular mechanisms of angiotensin II-mediated mitochondrial dysfunction: linking mitochondrial oxidative damage and vascular endothelial dysfunction. *Circ Res* 2008;**102**:488–496.
48. Stump CS, Short KR, Bigelow ML, Schimke JM, Nair KS. Effect of insulin on human skeletal muscle mitochondrial ATP production, protein synthesis, and mRNA transcripts. *Proc Natl Acad Sci U.S.A* 2003;**100**:7996–8001.
49. Birk AV, Liu S, Soong Y, Mills W, Singh P, Warren JD, Seshan SV, Pardee JD, Szeto HH. The mitochondrial-targeted compound SS-31 re-energizes ischemic mitochondria by interacting with cardiolipin. *J Am Soc Nephrol* 2013;**24**:1250–1261.
50. Kloner RA, Hale SL, Dai W, Gorman RC, Shuto T, Koomalsingh KJ, Gorman JH, 3rd, Sloan RC, Frasier CR, Watson CA, Bostian PA, Kypson AP, Brown DA. Reduction of ischemia/reperfusion injury with bendavia, a mitochondria-targeting cytoprotective peptide. *J Am Heart Assoc* 2012;**1**:e001644.
51. Dai DF, Chen T, Szeto H, Nieves-Cintron M, Kutyavin V, Santana LF, Rabinovitch PS. Mitochondrial targeted antioxidant peptide ameliorates hypertensive cardiomyopathy. *J Am Coll Cardiol* 2011;**58**:73–82.
52. Eirin A, Lerman A, Lerman LO. Mitochondria: a pathogenic paradigm in hypertensive renal disease. *Hypertension* 2015;**65**:264–270.